

## General Disclaimer

### One or more of the Following Statements may affect this Document

- This document has been reproduced from the best copy furnished by the organizational source. It is being released in the interest of making available as much information as possible.
- This document may contain data, which exceeds the sheet parameters. It was furnished in this condition by the organizational source and is the best copy available.
- This document may contain tone-on-tone or color graphs, charts and/or pictures, which have been reproduced in black and white.
- This document is paginated as submitted by the original source.
- Portions of this document are not fully legible due to the historical nature of some of the material. However, it is the best reproduction available from the original submission.

# Fluid Sloshing Characteristics in Spacecraft Propellant Tanks with Diaphragms

Steve Green<sup>1</sup>, Russell Burkey<sup>2</sup>, Flavia Viana<sup>3</sup>,  
Southwest Research Institute, San Antonio, Texas, 78238

James Sudermann<sup>4</sup>  
NASA, Kennedy Space Center, Florida, 32899

All spacecraft are launched from the Earth as payloads on a launch vehicle. During portions of the launch profile, the spacecraft could be subjected to nearly purely translational oscillatory lateral motions as the launch vehicle control system guides the rocket along its flight path. All partially-filled liquids tanks, even those with diaphragms, exhibit sloshing behavior under these conditions and some tanks can place large loads on their support structures if the sloshing is in resonance with the control system oscillation frequency. The objectives of this project were to conduct experiments using a full-scale model of a flight tank to 1) determine whether launch vehicle vibrations can cause the diaphragm to achieve a repeatable configuration, regardless of initial condition, and 2) identify the slosh characteristics of the propellant tank under flight-like lateral motions for different diaphragm shapes and vibration levels. The test results show that 1) the diaphragm shape is not affected by launch vibrations, and 2) the resonance-like behavior of the fluid and diaphragm is strongly affected by the nonlinear stiffness and damping provided by the diaphragm.

## Nomenclature

$B_{\theta,eff}$	=	effective torsional damping coefficient of the diaphragm and viscous effects
$F_T$	=	force exerted on tank
$g$	=	acceleration due to gravity (or thrust level)
$H_o$	=	position of 'stationary' fluid center of mass
$H_p$	=	pendulum hinge point location
$H_T$	=	position of tank structure center of mass
$K_{\theta}$	=	diaphragm torsional stiffness
$K_{\theta,eff}$	=	effective combined torsional stiffness of diaphragm and gravity effects
$L_p$	=	pendulum length
$\hat{M}_P$	=	apparent mass moment of the pendulum bob acting through the pendulum hinge point
$M_T$	=	moment applied to the tank
$m_T$	=	mass of tank structure
$m_o$	=	mass of 'stationary' portion of fluid
$m_p$	=	mass of 'moving' portion of fluid
$R_T$	=	tank radius
$\hat{W}_P$	=	apparent mass of the pendulum bob
$\ddot{x}_T$	=	tank acceleration
$\omega_n$	=	undamped natural frequency

<sup>1</sup> Staff Engineer, Mechanical and Fluids Engineering Department, 6220 Culebra Rd, AIAA Member.

<sup>2</sup> Senior Research Engineer, Mechanical and Fluids Engineering Department, 6220 Culebra Road, AIAA Non-Member.

<sup>3</sup> Research Engineer, Mechanical and Fluids Engineering Department, 6220 Culebra Road, AIAA Non-Member.

<sup>4</sup> Controls Analyst, ELV Control Systems Analysis, Mail Code VA-F3, AIAA Member.

$\Omega$  = excitation frequency  
 $\zeta$  = damping ratio

## I. Introduction

THE sloshing dynamics of liquids in spacecraft fuel tanks is a concern of spacecraft designers and mission planners. Spacecraft control systems and sensors can be influenced by sloshing fuel or by fuel simply not being in the expected center of gravity location. Spacecraft fuel slosh can also interact with the launch vehicle control system and cause unpredicted motions and reactions. Slosh effects can be categorized into two broad categories. The first category includes motions associated with surface oscillations caused by launch vehicle and spacecraft maneuvers and, if induced under an acceleration field, is usually some type of bulk fluid motion with a periodic component. The second category is slosh induced by interaction with a spinning or rotating spacecraft. This type of slosh can be bulk fluid motion and/or subsurface wave motion (currents) and almost always is periodic because of the spin. In either case, an unpredicted coupled resonance between the vehicle or spacecraft and the on-board fuel can have mission-threatening affects. This paper deals with the free-surface category of sloshing and how a diaphragm-type of propellant management device (PMD) affects the sloshing characteristics of the fluid.

The sloshing dynamics of fluids in containers have been the subject of many articles and books for several decades. One of the most widely used references on the subject is Abramson<sup>1</sup> and there was enough interest in the subject over the ensuing 30 years that Dodge<sup>2</sup> updated that early monograph. These two referenced works and the majority of the many articles in the open technical literature concerning fluid sloshing in tanks deal mainly with the dynamics of liquids with a free surface. Many spacecraft, however, use diaphragms to restrain the fluid movement and assist in the expulsion of the propellant from the tank. Diaphragms are a lightweight and effective means of controlling fluid position, damping free-surface oscillations, and efficiently expelling propellant from the tank. The sloshing behavior of these types of spacecraft tanks has been studied, but there is a shortage of information in the open literature regarding the fluid-structure interactions in tanks with diaphragms. Much of the work is proprietary or is contained in reports with a limited distribution. This paper attempts to shed light on some features of the lateral sloshing characteristics of a tank with a diaphragm PMD.

The motivation for this study was the observation of second-stage nozzle control oscillations in the launch vehicle for the Deep Impact mission. The nozzle control system oscillations were attributed to interactions with the lateral sloshing of the propellant in the Deep Impact spacecraft<sup>3</sup>. It should be noted that the spacecraft propellant mass was a small fraction of the total mass of the launch vehicle, which points to the impact that fluid sloshing can make. While this interaction was in no way threatening to the Deep Impact mission, it highlights the fact that sloshing effects cannot be considered negligible, even when a PMD is used.

The objectives of this investigation were as follows:

1. Determine the response of the diaphragm shape to simulated launch vibrations; in particular, determine whether the diaphragm can achieve some stable repeatable configuration after being subjected to launch vehicle vibrations.
2. Experimentally determine the slosh dynamic characteristics of a propellant tank under conditions similar to the launch phase and develop a mechanical model that simulates this behavior.

The basic approach will be to apply the well-known mechanical pendulum concept to the analysis of the test data and compare the model predictions to the test data. Out of convenience, the test program used a tank that was already available. The test article was a full-scale model of a tank used in the STEREO spacecraft. The aim of this program was not to address issues specific to the Deep Impact mission, and the use of the available tank does not invalidate the general conclusions arising from this investigation.

## II. Pendulum Analog to Fluid Sloshing

### A. Model Equations

In a partially-filled tank that is undergoing oscillatory lateral motion, the fluid imparts forces and moments on the tank walls. If the sloshing is of a low level such that there are no breaking waves at the fluid surface, then the mechanical dynamic effects of liquid sloshing can be well represented by a stationary mass and a pendulum. This mechanical analog is depicted in Fig. 1. The theory underlying this mechanical analog is well established (see

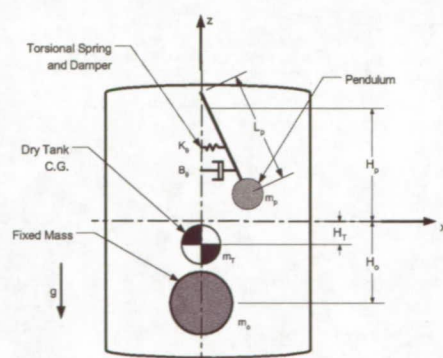


Figure 1. Pendulum Slosh Model Analog

Abramson<sup>1</sup>). The stationary mass represents the portion of the fluid that does not move relative to the tank, while the pendulum bob represents the sloshing portion of the fluid.

Gravity acts as a restoring force providing stiffness for the system and the energy dissipation of the fluid via viscous forces at the walls providing the damping. This concept is often extended to include the effects of a diaphragm enclosing the fluid surface. These effects are included as a torsional spring and damper in addition to those for the pendulum alone.

The equations of motion for the pendulum-diaphragm system undergoing forced oscillatory lateral motion can be developed to determine the external force required to execute the motion. This is expressed as:

$$\frac{F_T}{\ddot{x}_T} = m_T + m_o + m_p \left[ 1 + \frac{\Omega^2}{\omega_n^2 - \Omega^2 + i(2\zeta\Omega\omega_n)} \right] \quad [1]$$

$$\omega_n = \text{undamped natural frequency} = \left[ \frac{g}{L_p} + \frac{K_\theta}{m_p L_p^2} \right]^{1/2} = \left[ \frac{K_{\theta,eff}}{m_p L_p^2} \right]^{1/2}$$

$$\zeta = \text{damping ratio} = \left[ \frac{B_{\theta,eff}}{2\sqrt{K_{\theta,eff} m_p L_p^2}} \right]$$

The complex form of Eq. [1] is retained where  $i = \sqrt{-1}$ . Similarly, the moment required to maintain the tank in purely translational motion is given by:

$$\frac{M_T}{\ddot{x}_T} = m_T H_T + m_o H_o + m_p H_p \left[ 1 + \frac{\Omega^2}{\omega_n^2 - \Omega^2 + i(2\zeta\Omega\omega_n)} \right] - m_p L_p \left[ \frac{i(2\zeta\Omega\omega_n)}{\omega_n^2 - \Omega^2 + i(2\zeta\Omega\omega_n)} \right] \quad [2]$$

Note that the linear momentum equation, Eq. [1], is written in terms of a transfer function of force divided by acceleration. This has units of mass and the ratio will be referred to as an apparent mass. Likewise, the angular momentum equation, Eq. [2], is written in terms of transfer function of moment divided by acceleration. This has units of mass times length and will be referred to as an effective mass-moment.

## B. Model Parameter Extraction

The pendulum mechanical analog equations can be manipulated to provide a means of computing the pendulum model parameters from the measured forces and moments.

First, Eq. [1] can be rearranged to define the apparent slosh mass as follows:

$$\hat{W}_p = \frac{F_T}{\ddot{x}_T} - m_T - m_o = m_p \left[ 1 + \frac{\Omega^2}{\omega_n^2 - \Omega^2 + i(2\zeta\Omega\omega_n)} \right] \quad [3]$$

where  $\hat{W}_p$  is considered the apparent mass of the pendulum bob. This complex quantity is computed directly from the measured force and acceleration. This equation has features that make it useful for analyzing the data measured in a lateral slosh test. First, at high enough excitation frequencies, the real part of Eq. [3] should ideally be zero. The dry tank mass,  $m_T$ , is presumably known; so, at frequencies well above a resonance, Eq. [3], is used to estimate the stationary mass,  $m_o$ .

Near enough to a resonant frequency,

$$1 \ll \frac{\Omega^2}{\omega_n^2 - \Omega^2 + i(2\zeta\Omega\omega_n)}$$

so that Eq. [3] is simplified to

$$\hat{W}_p = m_p \frac{\Omega^2}{\omega_n^2 - \Omega^2 + i(2\zeta\Omega\omega_n)} \quad (\text{near resonance}) \quad [4]$$

Unruh et al.<sup>4</sup>, show that the real terms in Eq. [4] can be used in a least-squares method applied to measured values of  $\hat{W}_p$  to estimate values for  $m_p$  and  $\omega_n$ . The damping ratio,  $\zeta$ , is then computed using the imaginary terms. This method, however, assumes that the damping is low and there is significant amplification near the resonance peak.

The pendulum length is computed from the expression for the overall stiffness in the system,

$$\omega_n^2 = \frac{g}{L_p} + \frac{K_\theta}{m_p L_p^2} = \frac{K_{\theta,eff}}{m_p L_p^2} \quad [5]$$

For the case of a free-surface tank, the torsional stiffness of the diaphragm is not present ( $K_\theta=0$ ), and the pendulum length can be directly computed from the previously determined value for  $\omega_n$ . For the case of a tank with a diaphragm, it is necessary to conduct tests with two different fluids (or at two different gravity conditions) so that  $L_p$  and  $K_\theta$  can be simultaneously computed using Eq. [5] and the two independent sets of values for  $\omega_n$  and  $m_p$ .

Next, the angular momentum equation, Eq. [2], is rearranged to define the apparent mass moment as:

$$\hat{M}_p = \frac{M_T}{\ddot{x}_T} - m_T H_T - m_o H_o = m_p H_p \left[ 1 + \frac{\Omega^2}{\omega_n^2 - \Omega^2 + i(2\zeta\Omega\omega_n)} \right] - m_p L_p \left[ \frac{i(2\zeta\Omega\omega_n)}{\omega_n^2 - \Omega^2 + i(2\zeta\Omega\omega_n)} \right] \quad [6]$$

where  $\hat{M}_p$  can be considered the apparent mass moment of the pendulum bob acting through the pendulum hinge point. Again, at high enough frequencies, the real part of Eq. [6] is ideally zero. If the dry tank center of mass position is known, then Eq. [6] is applied to the high-frequency measurements to estimate the value of the stationary mass center of mass position,  $H_o$ . It is then convenient to use the real parts of Eq. [6] for the near-resonance measurements to compute the value of  $H$ , since all of the other terms are now known.

### III. Test Tank

All testing was performed with a tank geometrically similar to the STEREO hydrazine fuel tanks. The tank simulator, Fig. 2, has clear acrylic hemispherical domes (for flow visualization) with an aluminum cylindrical center section. The aluminum cylinder holds the flight-like diaphragm supplied by the flight tank vendor. The tank was designed and fabricated to simulate the internal features of the actual STEREO flight hardware. The tank has an inside diameter of 16.5 inches and the dome centers are separated by 3.415 inches. The diaphragm is held slightly toward the gas side of the tank mid-plane.

### IV. Diaphragm Settling Tests

#### A. Test Setup

A series of tests were performed to determine if there is a naturally preferred diaphragm shape that is achieved as a result of vibrations experienced during launch. This preferred diaphragm shape search was conducted with the STEREO Tank Simulator installed in a fixture mounted to the biaxial (lateral and vertical) hydraulic shaker tables in the SwRI Environmental Testing Laboratory. A picture of the diaphragm settling test setup is shown in Fig. 3. The

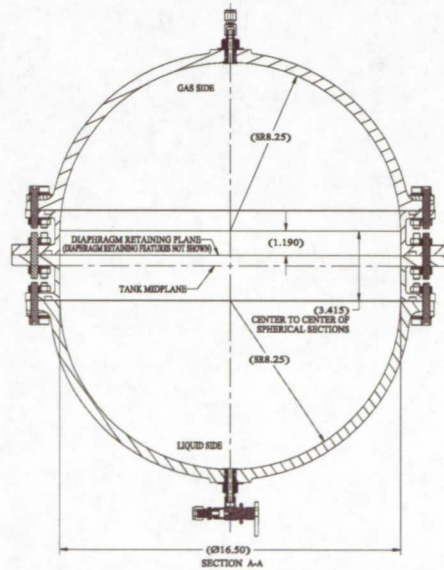


Figure 2. STEREO Tank Simulator

top acrylic hemisphere of the STEREO Tank Simulator was removed for the entire test series to allow convenient manipulation of the diaphragm shape. The test fixture shown in Fig. 3 is a dynamometer that was used in spinning slosh tests of this tank in a separate project. The dynamometer is used here simply as a means of holding the tank on the shaker. A single fill level of 61% was used in the diaphragm settling tests.

The prescribed motion of the biaxial shaker table was controlled to match a shock spectrum that was developed to approximately simulate the more severe portions of the launch vehicle vibration environment while also considering the capabilities of the shaker table. An example of the input spectrum and the table response spectrum are shown in Fig. 4.

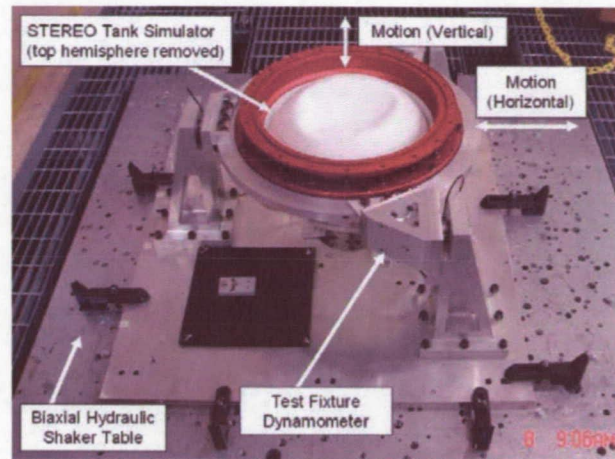


Figure 3. Diaphragm Settling Test Setup

### B. Test Results

Tests were conducted with the diaphragm in each of the different initial shapes shown schematically in Fig. 5. The ridge shape was formed to be both in-plane and out-of-plane with respect to the lateral motion so that five different initial diaphragm configurations were tested. Each initial diaphragm shape condition was subjected to the same representative biaxial launch level random vibration spectrum and the diaphragm motion and final configuration were videoed and photographed. No dynamometer force sensor data were collected during the preferred diaphragm shape search testing.

The final diaphragm shape after the random vibration spectrum showed no changes from the initial diaphragm shape for all of the shapes tested. Therefore, it appears that the diaphragm tends to remain in its original shape when subjected to a representative launch level random vibration spectrum rather than move to a single preferred diaphragm shape.

This observation is strictly valid for only this particular tank and diaphragm combination. Testing conducted with small-scale models of hydrazine tanks in a drop tower (see Chatman et al.<sup>4</sup>) also shows that the initial diaphragm is resistant to change after the severe decelerations used in spinning drop tests. Recent testing, however, with a full-scale model of a 23-inch diameter tank has demonstrated that some diaphragm shapes are not resistant to alteration under spinning loads. This limited observational evidence indicates that diaphragm shape stability is dependent on tank size. Furthermore, since the

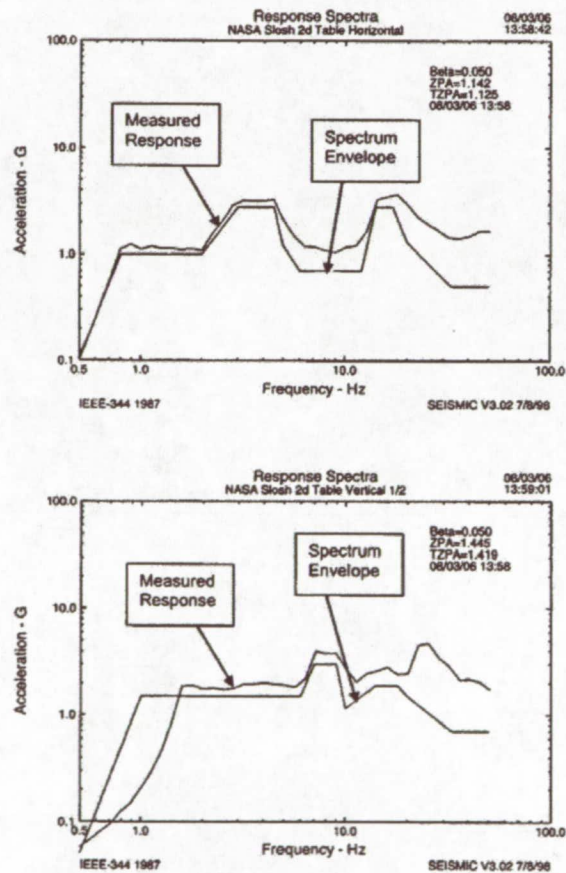


Figure 4. Biaxial Shock Spectra for Diaphragm Settling Tests

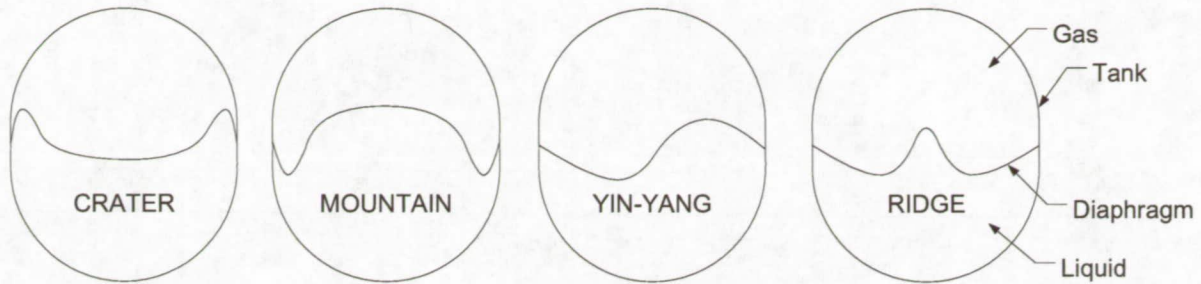


Figure 5. Diaphragm Shapes

flight tank diaphragms are not visible when the tank is filled, the diaphragm shape that exists when the spacecraft is launched is largely unknown and cannot be manipulated with confidence into a known shape by simple motions or vibrations of the tank.

## V. Slosh Tests

### A. Test Setup

The lateral slosh testing was conducted by imposing a forced sinusoidal displacement on the STEREO tank simulator and measuring the resulting lateral force and moment. A photograph of the lateral slosh test setup with the STEREO simulator tank is shown in Fig. 6. The STEREO Tank Simulator was suspended from a fixed steel frame using spherical bearings and thin aluminum tubes. The frame was made tall enough so that the suspended tank executed nearly pure lateral motion for the small displacements (less than +/- 5") experienced in this test program.

The forced sinusoidal displacement was provided by a hydraulic cylinder. The testing was conducted at uniform peak acceleration over the frequency range of interest. The hydraulic cylinder was controlled in a closed loop feedback mode with a control accelerometer mounted on the cylinder rod clevis as the feedback sensor.

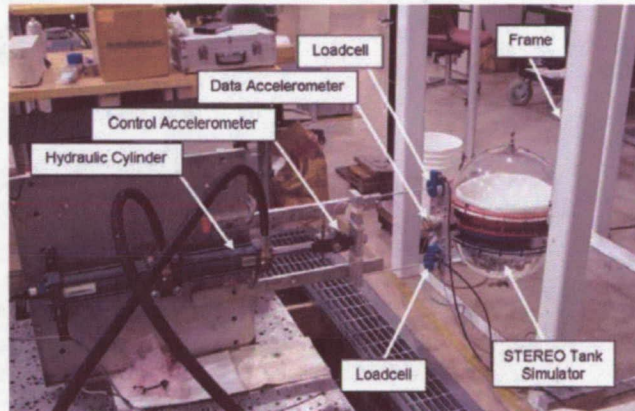


Figure 6. Lateral Slosh Test Setup

Two commercially available single-axis, strain-gage type loadcells were installed as part of the linkage between the hydraulic cylinder and suspended tank. The two loadcells were located symmetrically about the geometric center of the tank in a vertical plane passing through the axis of the tank. The total force in the lateral displacement direction and the total moment about the transverse direction are given by the sum and difference of the two force sensor outputs, respectively.

The tank acceleration was measured with an accelerometer mounted to a plate attached to the tank in the linkage between the hydraulic cylinder and suspended tank. The sensor has a useful frequency range of 0.025 Hz to 800 Hz.

The force and acceleration signals were collected with a PC-based data acquisition system (DAS). The DAS included a 16-bit analog to digital data acquisition card. The DAS software was developed in the LabVIEW (version 7.1) programming language. The data were collected at a rate of 300 samples per second.

### B. Model Verification – Free-Surface Tank

Some tests were conducted with the STEREO Tank Simulator without the diaphragm in spite of the fact that the STEREO tanks are not intended to fly without a diaphragm in place. The purpose of these tests was to demonstrate and at least qualitatively validate the data analysis methodology described above. These tests were conducted with deionized water at the 61% nominal fill level used throughout this test program.

The test data are shown in Fig. 7 and Fig. 8. The data are presented in terms of the magnitude and phase of the transfer function for apparent mass and mass moment defined in Eqs. [1] and [2]. It is seen that there is a high, narrow peak in the curves indicating a sharp resonance with low damping. The resonance amplification factor is about 16 for the apparent mass and about 17 for the apparent mass-moment. The data analysis method described above is well suited to this type of data. The equations outlined above can be used to solve directly for all of the

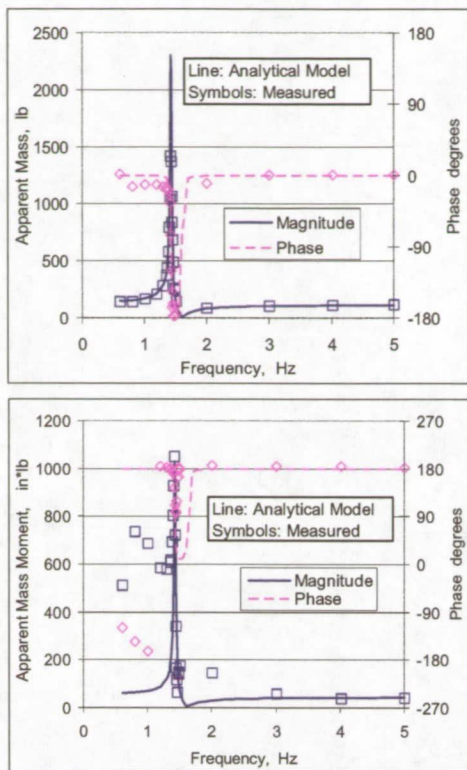


Figure 7. Free Surface Tank Dynamic Response

used with the crater shape to investigate the possible nonlinear stiffness and damping effects of the diaphragm. The in-plane and out-of-plane ridge shapes were subjected to only the 0.25-g excitation. Water and perfluorohexane ( $CF_6$ , the specific gravity  $\sim 1.67$ ) were used as the test fluids so that the diaphragm stiffness could be separated from the overall stiffness in accordance with Eq. [5] above. For the sake of brevity, only the results for the water tests will be shown in the graphs below. The key results of the tests with  $CF_6$  will be described as appropriate.

Table 1. Free-Surface Tank SLOSH Model Results

SLOSH MODEL PARAMETER	61% Fill Level	
	Meas.	Theory
Total Liquid Mass, lb	67	
Pendulum Mass, $m_p$ , lb	28.9	27.8
Natural Frequency, $\omega_n$ , Hz	1.43	1.45
Damping Ratio, $\zeta$	0.0054	0.0016
Pendulum Length, $L_p$ , in	4.81	4.66
Hinge Point, $H_p$ , in	-0.45	-0.66
Stationary Mass Position, $H_o$ , in	-1.7	-1.5

### 1. Crater Shape Tests

The test results for the crater shape with water are summarized in Fig. 8. The test data are indicated by the symbols in these graphs. These test data are used in conjunction with the  $CF_6$  test results to derive the pendulum model parameters as described above. The pendulum model results are compared to the test data where the model results are shown as the solid lines in the graphs.

The resonance peaks for the diaphragm cases are obvious here, although they are much broader and shorter than those for the free-surface tank. The corresponding peaks in the curves for the  $CF_6$  test results occur at lower frequencies than for water. This is expected because the density of  $CF_6$  is greater than that of water.

The measured data and the predictions are in reasonable agreement for this diaphragm shape. The resonance peaks are sharp enough that the parameter extraction methodology described above could be used to provide initial

pendulum model parameters. Also, for this case of a free-surface tank, the sloshing characteristics can be computed accurately by the SLOSH code described by Dodge<sup>2</sup>.

The experiment data analysis results are summarized along with the SLOSH code predictions in Table 1. The hinge point and center of mass positions are defined with respect to the geometric center of the tank and the natural frequency is that for the laboratory 1-g environment. There is good agreement between the parameters obtained from the test measurements and those provided by the SLOSH code predictions with one notable exception. The measured damping is greater than the predicted value. This is not surprising because the tank has a protrusion near its equator that is used to clamp the diaphragm. This device was left in place during the testing and was not included in the SLOSH code predictions.

The magnitudes of the predicted mass and moment transfer functions are in close agreement with the measured values, except in the low-frequency range for the mass-moment. The agreement of the predicted and measured phases is reasonably good around the resonance frequency. It should be noted that the slosh model parameters described in Table 1 were computed using the appropriate simplification of the overall transfer functions described above in a tight range of frequencies that bracket the resonant frequency. The graphs of the predicted transfer functions, however, are for the complete expressions given in Eqs. [1] and [2].

### C. Diaphragm Tests

The lateral slosh tests of a tank with a diaphragm in place were conducted for the crater, in-plane ridge, and out-of-plane ridge shapes. Three different sinusoidal excitation accelerations were



estimates for the pendulum model parameters for both fluids. These initial values were used as the starting point in the following method to arrive at slosh model parameters applicable to both fluids, as appropriate.

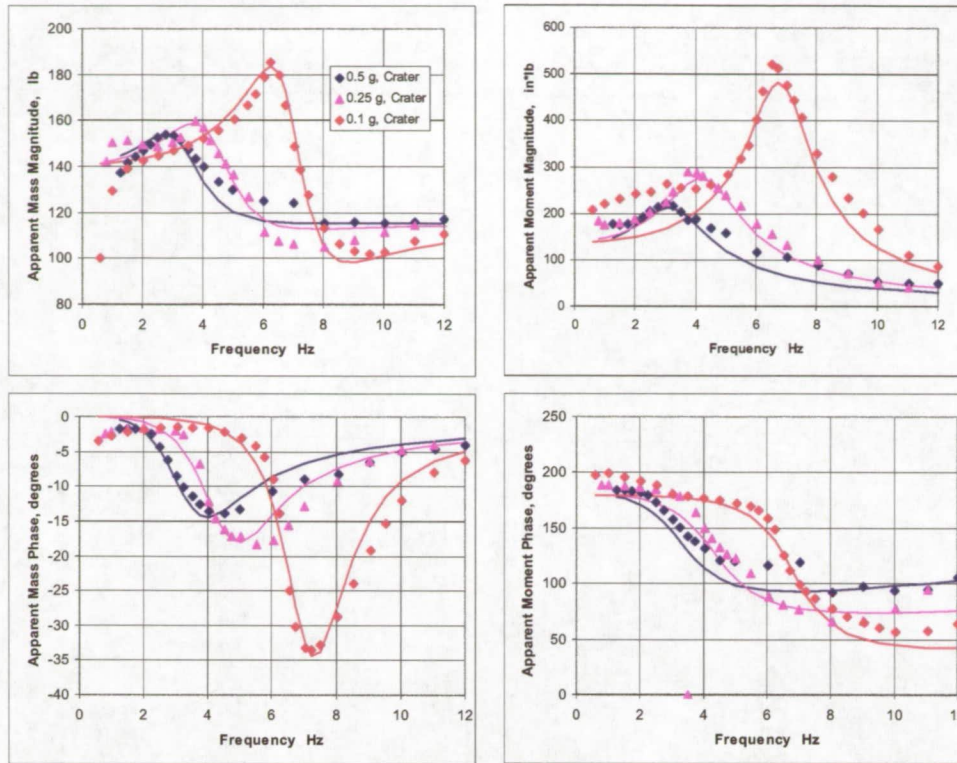


Figure 8. Fluid Sloshing Behavior with Water for Crater Diaphragm Shape

First, as in the case of the free-surface tank, the high-frequency measurements were used in conjunction with Eq. [3] to estimate the stationary mass. A value of  $m_o$  was selected that provided a value of  $0.0 \pm 0.1$  lb for the real term in Eq. [3]. Next, the initial guesses of the natural frequency and damping were adjusted such that the characteristics of the measured data near the resonance frequency were matched reasonably well in accordance with a qualitative inspection of the graphs during the selection process. The third step in the process was the simultaneous solution for  $L_p$  and  $K_\theta$  with Eq. [5]. Next, the high-frequency data for the apparent mass-moment were used to choose a value for  $H_o$  that yielded a value of  $0.0 \pm 1.0$  in.lb for the real term in Eq. [6]. Finally, Eq. [6] was used to provide an initial estimate for  $H_p$  near resonance. This value was iterated until there was reasonable agreement between the measured and predicted values for the apparent mass-moment for both fluids over the entire frequency range. It is assumed that, similar to the reasoning that the pendulum length should be the same for both of the fluids, the hinge point location is the same for each of the fluids. The results of the model parameter extraction procedure for the crater shape tests are summarized in Table 2.

It was discovered that the peak mass moment is under-predicted for the water and over-predicted for the  $CF_6$ . This is a result of forcing the hinge points for the two fluids to be identical. The actual case may be that the diaphragm interacts differently with the two fluids such that the effective pendulum length, stiffness, and hinge point may not be identical for the two cases. Nonetheless, this model assumption is retained in this analysis approach.

The resonance frequencies decrease and the resonance peaks are lower and broader as the excitation level increases. This is an indication that the fluid/diaphragm interaction is excitation dependent. Furthermore, this combination of fluids yielded results that could not be combined in Eq. [5] to provide meaningful values for the pendulum length and the effective rotational stiffness for the 0.5-g excitation level. That is, the combination of pendulum masses and natural frequencies yield a negative value for the pendulum length. It was observed (and recorded on video) that the diaphragm motions were different for the two fluids at this excitation level. The diaphragm motion was more pronounced with the perfluorohexane than when water was in the tank. The large motions and the excitation-dependent behavior of the diaphragm all indicate that the response of the fluids and

diaphragm are highly nonlinear for this excitation. It is not surprising that a model based on the assumptions of linear behavior is not entirely successful here.

**Table 2. Crater Diaphragm Slosh Model Parameters**

*These values are obtained by fitting the pendulum model to the measured data*

SLOSH MODEL PARAMETER	0.10 g		0.25 g		0.50 g	
	H <sub>2</sub> O	CF <sub>6</sub>	H <sub>2</sub> O	CF <sub>6</sub>	H <sub>2</sub> O	CF <sub>6</sub>
Total Liquid Mass, lb	67	110	67	110	67	110
Pendulum Mass, $m_p$ , lb	25	50	25	47	25	45
Natural Frequency, $\omega_n$ , Hz	6.9	5.1	4.5	3.6	3.5	2.1
Damping Ratio, $\zeta$	0.15	0.20	0.30	0.33	0.38	0.55
Pendulum Length, $L_p$ , in	2.2		2.1		2.1*	
Diaphragm Stiffness, $K_\theta$ , in.lbf/rad	543		174		86**	
Hinge Point, $H_p$ , in	-5.5		-5.5		-4.8	
Stationary Mass Position, $H_o$ , in	-0.5		-0.6		-0.8	

\*Assumed approximately equal to the values at 0.1 g and 0.25 g.

\*\*Computed from only the water results.

## 2. Ridge Shape Tests

The in-plane and out-of-plane ridge shapes for the diaphragm were tested. The diaphragm shapes for the water-filled tank were similar, except that the central ridge was slightly broader than with the perfluorohexane. The difference was apparently caused by the fluid properties, because the shapes for the two fluids could not be made identical in this respect. The single excitation level for the in-plane ridge tests was 0.25 g.

The test data are summarized in terms of apparent mass and apparent mass moment in Fig. 9. Only the iterative method of extracting the slosh model parameters was useful here. Also, as in the case of the 0.5-g excitation for the crater shape, the combination of pendulum masses and natural frequencies for the ridge shapes at 0.25-g excitation

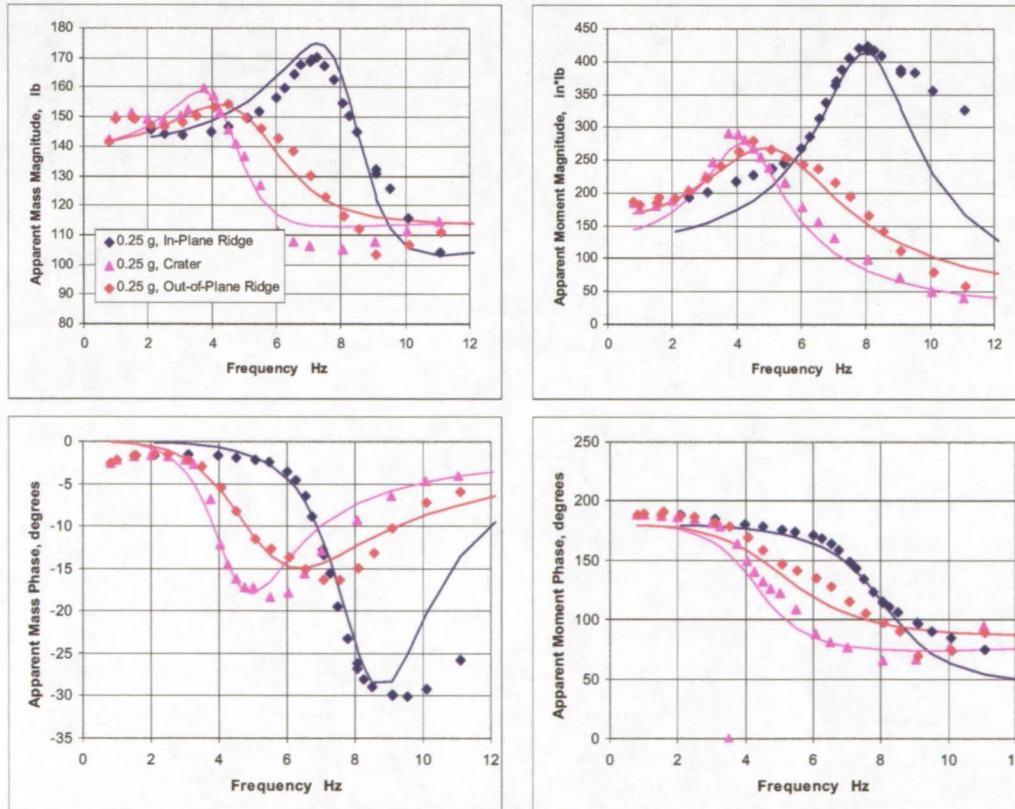


**Figure 9. Fluid Sloshing Behavior with Water for Three Diaphragm Shapes at 0.25-g Excitation**

yields a negative value for the pendulum length. It was observed (and recorded on video) that the diaphragm motions were different for the two fluids at this excitation level. The diaphragm motion was more pronounced with the CF<sub>6</sub> than when water was in the tank. This difference in dynamic response is linked to the problem of obtaining consistent values of pendulum length and diaphragm stiffness.

The resonance frequency and amplification are greater for the in-plane shape than for both out-of-plane and crater shapes. There is reasonable agreement between the measured and predicted values for these tests around the resonance peaks, but the agreement is not as good for the high-frequency parts of the range. There is an anomaly in the moment test results for the water case in that the mass moment for the high-frequency portions of the data is greater than the moment at low frequency. Other than this anomaly, the shape and peak of the mass moment resonance characteristics are predicted well.

The computed slosh model parameters for the two ridged diaphragm shapes are summarized in Table 3.

**Table 3. Ridge Diaphragm Slosh Model Parameters**

*These values are obtained by fitting the pendulum model to the measured data.*

SLOSH MODEL PARAMETER	Out-of-plane		In-Plane	
	WATER	CF <sub>6</sub>	WATER	CF <sub>6</sub>
Total Liquid Mass, lb	67	110	67	110
Pendulum Mass, $m_p$ , lb	27	45	25	50
Natural Frequency, $\omega_n$ , Hz	5.5	2.8	8.2	3.8
Damping Ratio, $\zeta$	0.4	0.55	0.18	0.41
Pendulum Length, $L_p$ , in	2.2*		2.2*	
Diaphragm Stiffness, $K_\theta$ , in.lbf/rad	345(H <sub>2</sub> O) / 76(CF <sub>6</sub> )**		777(H <sub>2</sub> O) / 247(CF <sub>6</sub> )**	
Hinge Point, $H_p$ , in	-6.0		-5.8	
Stationary Mass Position, $H_o$ , in	-0.6		-0.3	

\*Assumed approximately equal to the values for the crater shape.

\*\*Computed from the assumed value of  $L_p$ .

## VI. Conclusions

A study of the dynamic characteristics of the STEREO spacecraft tanks under two types of excitation was conducted. The tank simulator used here closely matched the internal features of the flight tank. A tank fill level of 61% was used in the test program and the test fluids were deionized water and perfluorohexane.

In the first set of tests, the tank was subjected to simultaneous bilateral vibrations along the tank axis and a transverse axis. The objective of these tests was to determine whether the tank diaphragm would achieve a stable, repeatable configuration after being subjected to motions equivalent to those of a launch vehicle. The diaphragm was manipulated into different initial shapes prior to being shaken. It was found that shaking the tank would not significantly alter the initial diaphragm shape. The implication of this (at least for this particular tank) is that analysts cannot assume that the diaphragm will achieve a repeatable configuration during launch.

In the second set of tests, the tank was subjected to lateral excitations to determine the appropriate parameters for a mechanical pendulum analog to the sloshing behavior for the prediction of forces and moments on the tank walls. Tests were conducted for combinations of three different diaphragm shapes and three different excitation levels. Two test fluids having different densities were required to separate the effects of the diaphragm stiffness and the pendulum length on the net effective stiffness of the system.

The overall conclusion of this test program is that the pendulum slosh model geometric parameters are relatively insensitive to variations in diaphragm shape and excitation level. That is, the following were obtained for the pendulum model of the tested tank:

- Pendulum Length:  $0.25 \leq \frac{L_p}{R_T} \leq 0.27$
- Hinge Point Location:  $0.58 \leq \frac{H_p}{R_T} \leq 0.73$
- Fixed Mass Location:  $0.06 \leq \frac{H_o}{R_T} \leq 0.10$

The mass of the pendulum is also relatively insensitive to excitation and shape, but the pendulum mass as a fraction of the total liquid mass is fluid dependent. This is not the case for free-surface tanks, but it was observed that for the large excitations used here (e.g.,  $\geq 0.25g$ ), the test fluids interacted differently with the diaphragm. Finally, the other dynamic properties of the tank varied strongly with excitation level. The diaphragm stiffness is inversely proportional to the excitation level and the damping ratio is directly proportional to the excitation level. The nonlinear behavior of the diaphragm cannot be easily predicted and presents a challenge to modeling the diaphragm dynamic effects. It seems that the most expedient resolution to this challenge will be testing such as that conducted here.

Finally, it should be noted that the natural frequency values reported here correspond to the 1-g test conditions. These values must be corrected for the expected thrust levels of the spacecraft, under flight conditions.

### Acknowledgments

The authors would like to acknowledge Dr. Isam Yunis, formerly of NASA-KSC, and Mr. Daniel Pomerening of Southwest Research Institute for their assistance in specifying the bilateral shaker table shock spectrum for simulating a typical launch vehicle vibration environment.

### References

- <sup>1</sup>Abramson, H. N. (ed.), "The Dynamic Behavior of Liquids in Moving Containers," NASA SP-106, 1966.
- <sup>2</sup>Dodge, F. T., The New "Dynamic Behavior of Liquids in Moving Containers," Southwest Research Institute.
- <sup>3</sup>Walker, C. F., NASA-Kennedy Space Center, Personal Communication.
- <sup>4</sup>Unruh, J. F., Kana, D. D., Dodge, F. T., Fey, T. A., "Digital Data Analysis Techniques for Extraction of Slosh Model Parameters," *AIAA Journal of Spacecraft and Rockets*, Vol. 23, No. 2, March-April, 1986, pp 171-177.
- <sup>5</sup>Chatman, Y., Schlee, K., Gangadharan, S., and Ristow, J. Embry-Riddle Aeronautical University, Sudermann, J. E. and Walker, C.F., NASA, Kennedy Space Center, Hubert, C., Hubert Astronautics, Inc., "Modeling and Parameter Estimation of Spacecraft Fuel Slosh with Diaphragms Using Pendulum Analogs," 30th Annual Guidance, Navigation and Control Conference, American Astronautical Society, February 2007.